FACTA UNIVERSITATIS
Series: **Mechanics, Automatic Control and Robotics** Vol.4, N° 16, 2004, pp. 85 - 99

IMPLICIT STRESS INTEGRATION ALGORITHM FOR GURSON MODEL IN CASE OF LARGE STRAIN SHELL DEFORMATION

UDC 518.12:620.10:531.3(045)

Miloš Kojić, Ivo Vlastelica, Miroslav Živković

Faculty of Mechanical Engineering, University of Kragujevac, Serbia

Abstract. *An implicit stress integration procedure for the Gurson material model – the metal plasticity with volumetric plastic strain – and for large strain shell deformation is presented in the paper. The stress calculation is based on the governing parameter method (GPM), with the increment of the mean plastic strain Δe^P_m taken as the governing parameter. The shell condition (the zero stress through shell thickness) is satisfied at the end of time (load) step and the problem is reduced to solving the nonlinear equation with respect to Δe^P_m. The procedure is robust and computationally efficient. The conversion of the shell solution to the general 3-D conditions provides implementation of the 3-D consistent tangent elastic-plastic matrix.*
The small strain stress calculation procedure is extended to the large strain shell deformation. The multiplicative decomposition of the deformation gradient and the logarithmic strains are employed. This extension is based on a simple implementation of the 3-D kinematics relations to the shell conditions.
The solved numerical examples illustrate accuracy and the effectiveness of the proposed procedure.

Key words: *Gurson model, Implicit stress integration, the governing parameter method, large strain shell deformation, multiplicative decomposition of deformation gradient, logarithmic strains.*

1. INTRODUCTION

The development of material models that adequately represent the material behavior have been one of the fundamental tasks of the experimental and theoretical investigations, starting from Tresca 1884 [1], von Mises 1913 [2] and Hill 1950 [3]. The improvements of the earlier material models and formulation of the new ones last over decades and continue today. The description of various constitutive models, with emphasis to the geological materials, is given in [4]-[7], among others. Metal plasticity, viscoplasticity and creep models are described in, for example, [8]-[11]. We will further describe in detail a model for porous metal, introduced by Gurson [12] and modified by Tvergaard [13] and [14].

Received September 20, 2003

On the other hand, the developments of the numerical methods for the accurate calculation of the material response with the use of the material models, have become a very important field in the computational mechanics community, especially within the finite element method (FEM). First methods of solving elastic-plastic deformation of metals were of the iterative type (successive elastic solutions) [15], [8]. The first methods within the displacement based FE procedures were explicit (e. g. [10]), and later, in the 80' s, the implicit methods were developed. The implicit methods of stress integration in time step for inelastic material models ensure higher accuracy and, with calculation of the consistent tangent module, provide a dramatic improvement of the convergence rate with respect to the explicit methods. The implicit stress integration procedures are described in [16] and [17] for a number of material models. A review of the stress integration procedures is presented in [18].

An algorithm for implicit stress integration of the Gurson model in case of general 3-D small and large strain deformations is proposed in [19]. The algorithm is based on the governing parameter method (GPM) [20], which is a generalization of the effective-stress-function algorithm developed for thermoplastic and creep deformation of metals [21], [22]. Here we generalize the procedure proposed in [19] to shell (plane stress) conditions for small and large strains. For the completeness of this work, we further summarize the basic expressions that describe the Gurson model.

According to [12]-[15] the yield condition $f_y = 0$ for the Gurson model has the form

$$f_y = 1/2\,\mathbf{S}\cdot\mathbf{S} + \frac{1}{3}\left[2f^* q_1 \cosh\left(\frac{3q_2\sigma_m}{2\sigma_y}\right) - 1 - q_3^2 f^{*2}\right]\sigma_y^2 = 0 \tag{1}$$

where σ_y is the yield stress of the material, σ_m is the mean stress, f^* is a function of the void volume fraction (porosity) f; q_1, q_2 and q_3 are material constants, and

$$\mathbf{S}\cdot\mathbf{S} = S_{ij}S_{ij} \tag{2}$$

Here S_{ij} are the components of the stress deviator, and summation on the repeated indices is assumed (i, j = 1,2,3). The function f^* of the void volume fraction is given by

$$f^* = \begin{cases} f & \text{for } f \le f_c \\ f_c + K_f(f - f_c) & \text{for } f \ge f_c \end{cases} \tag{3}$$

where f_c is the critical void volume fraction when the onset of rapid volume coalescence begins, and

$$K_f = \frac{1/q_1 - f_c}{f_f - f_c} \tag{4}$$

Here f_f is value of f at material failure. Then we have $f^* = 1/q_1$, and from (1) follows (for $q_1 = q_3$) that the effective stress $\bar{\sigma} = (3/2S_{ij}S_{ij})^{1/2} = 0$ for $\sigma_m = 0$. Note that in case of $f^* = 0$ the yield condition (1) reduces to the von Misses yield condition with isotropic hardening behaviour.

In general, the rate of change of porosity can be written as [23]

$$\dot{f}_G = \dot{f}_G + \dot{f}_N + \dot{f}_C \tag{5}$$

where $\dot{f}_G, \dot{f}_N,$ and $\dot{f}_C$ correspond to the void growth, nucleation and coalescence, respectively. Assuming that the material matrix is practically incompressible and neglecting the elastic part of the void volume, the rate of void volume growth $\dot{f}_G$ can be expressed as

$$\dot{f}_G = (1-f)\dot{e}_V^P \tag{6}$$

where $\dot{e}_V^P$ is the plastic volumetric strain rate. If the nucleation of voids is dominated by the maximum normal stress, the rate of void nucleation $\dot{f}_N$ can be written in the form [24], [25]

$$\dot{f}_N = \frac{\hat{K}}{\sigma_y}(\dot{\sigma}_y + \dot{\sigma}_m) \tag{7}$$

where $\hat{K}$ is a dimensionless material parameter. This parameter can also be expressed in an analytical form that involves the yield stress σ_y and the mean stress σ_m, obtained through the statistical distribution of σ_y and σ_m. In case of nucleation dominated by the plastic strain, $\dot{f}_N$ can be written as [25]

$$\dot{f}_N = A\dot{\bar{e}}^P \tag{8}$$

where A can be either a material constant, or it can be chosen such that the void nucleation follows a normal distribution. In the latter case the coefficient A is

$$A = \frac{a_N}{s_N\sqrt{2\pi}}\exp\left[-\frac{1}{2}\left(\frac{\bar{e}^P - \bar{e}_N}{s_N}\right)^2\right] \tag{9}$$

where a_N is the amplitude, s_N is the standard deviation, $\bar{e}^P$ is the accumulated effective plastic strain, and $\bar{e}_N$ is the mean effective plastic strain of the normal distribution of the void nucleation. Finally, the rate of void coalescence $\dot{f}_C$ is proportional to the effective plastic strain rate, as it is $\dot{f}_N$ in equation (8), i.e.

$$\dot{f}_C = B\dot{\bar{e}}^P \tag{10}$$

The paper is organized as follows. In the next section we present the stress integration procedure for the shell small strain conditions, and then extend it to the large strain deformation in Section 3. Numerical examples are given in Section 4 and, finally, some concluding remarks are given in Section 5.

2. STRESS INTEGRATION PROCEDURE

We consider a shell deformation under the assumption of small strains. The basic geometry of shell finite element is shown in Fig.1 [26]-[28]. The position vector ${}^t\mathbf{X}$ at time "t" of a material point can be expressed as

$$ {}^t\mathbf{x} = h_k \, {}^t\mathbf{X}^k + \frac{t}{2} h_k a_k \, {}^t\mathbf{V}_n^k \tag{11} $$

where ${}^t\mathbf{X}^k$ are the position vectors of nodal points, $h_k(r,s)$ are the isoparametric interpolation functions of the in-plane natural coordinates r,s; ${}^t\mathbf{V}_n^k$ are the shell unit normal vectors, t is the natural coordinate in the shell normal direction, and $k = 1,...,N$ are the node numbers. The increment of the displacement vector $\Delta\mathbf{u}$ in time step Δt is

$$ \Delta\mathbf{u} = h_k \Delta\mathbf{U}^k + \frac{t}{2} a_k h_k (\Delta\boldsymbol{\varphi}^k \times {}^t\mathbf{V}_n^k) \tag{12} $$

where $\Delta\mathbf{U}^k$ are the nodal point displacement increments, and $\Delta\boldsymbol{\varphi}^k$ are the increments of rotations.

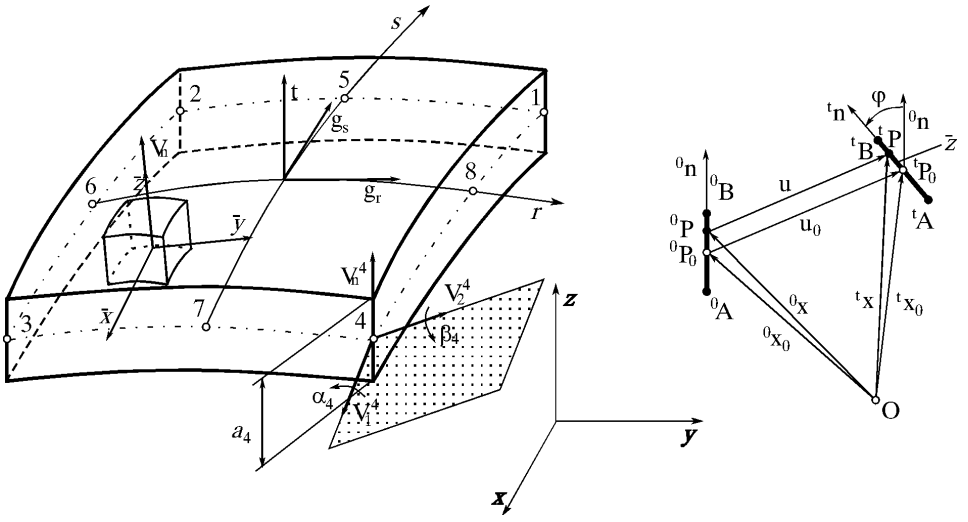

Fig. 1. Geometry and basic kinematics of shell finite element

Using the relation

$$ {}^{t+\Delta t}\mathbf{x} = {}^t\mathbf{x} + \Delta\mathbf{u} \tag{13} $$

we have that the coordinates ${}^t x_i$, ${}^{t+\Delta t}x_i$ and the displacement increments Δu_i are expressed in terms of the nodal point values and the natural coordinates r, s, t. Therefore, by the proper differentiation we can find the strains in the global coordinate system

$$(e_{glob})_{ij} = \frac{1}{2}\left(\frac{\partial u_i}{\partial x_j} + \frac{\partial u_j}{\partial x_i} \right) \tag{14}$$

for a given position (time).

The crucial condition in the shell analysis is that the normal stress through the shell thickness must be equal to zero. Hence, in the stress calculation we must satisfy the condition

$$^{t+\Delta t}\sigma_{zz} = 0 \tag{15}$$

where the local z-axis is in the direction of the shell normal. It follows that we have to perform the stress integration in the local shell coordinate system. We further assume that the strains $^{t+\Delta t}e_{ij}$, obtained by the tensorial transformation of the components (14), are known. For simplicity of writing we denote by x, y, z the local shell Cartesian coordinate system.

In order to develop the computational procedure for the stress calculation, we first define the incremental relations for the increments of plastic strains $\Delta\mathbf{e}^P$ and for the porosity Δf. From the flow rule

$$\Delta\mathbf{e}^P = \Delta\lambda \frac{\partial\, ^{t+\Delta t}f_y}{\partial\, ^{t+\Delta t}\boldsymbol{\sigma}} \tag{16}$$

and with use of (1), there follow increments of the mean strain Δe^P_m and of the deviatory strains $\Delta e'^P$,

$$\Delta e^P_m = \frac{\Delta\lambda}{3}\ ^{t+\Delta t}f'_y \tag{17}$$

$$\Delta e'^P_{ij} = \Delta\lambda\, ^{t+\Delta t}S_{ij} \tag{18}$$

where

$$^{t+\Delta t}f'_y = \frac{\partial^{t+\Delta t}f_y}{\partial\sigma_m} = q_1 q_2\, ^{t+\Delta t}\sigma_y\, ^{t+\Delta t}f^* \sinh\left(\frac{3q_2\, ^{t+\Delta t}\sigma_m}{2\, ^{t+\Delta t}\sigma_y} \right) \tag{19}$$

We write (5) in the incremental form and use (6), (8) and (10) to obtain

$$\Delta f = 3(1-\,^{t+\Delta t}f)\Delta e^P_m + (A+B)\Delta\bar{e}^P \tag{20}$$

If the evolution equation (7) is used instead (8), we have

$$\Delta f = 3(1-\,^{t+\Delta t}f)\Delta e^P_m + \frac{\hat{K}}{^{t+\Delta t}\sigma_y}(\Delta\sigma_y + \Delta\sigma_m) + B\Delta\bar{e}^P \tag{21}$$

In further derivations we will employ (20), with the use of A instead $A + B$. From (20) we obtain

$$\Delta f = [3(1-\,^{t}f)\Delta e^P_m + A\Delta\bar{e}^P]/(1+3\Delta e^P_m) \tag{22}$$

It is further assumed that the equivalence of plastic work is applicable [29]. Using the general loading and uniaxial loading conditions, we obtain

$$\boldsymbol{\sigma}\cdot\dot{\mathbf{e}}^{P}=(1-f)\sigma_{y}\dot{\bar{e}}^{P} \tag{23}$$

Written for the end of time step, this equation has the form

$${}^{t+\Delta t}f_{e}=\Delta\lambda^{t+\Delta t}\mathbf{S}\cdot{}^{t+\Delta t}\mathbf{S}+3^{t+\Delta t}\sigma_{m}\Delta e_{m}^{P}-(1-{}^{t+\Delta t}f)^{t+\Delta t}\sigma_{y}\Delta\bar{e}^{P}=0 \tag{24}$$

where the relation (18) is used

In the summary of the basic relations, we state that the yield condition at the end of time step must be satisfied, i. e.

$${}^{t+\Delta t}f_{y}({}^{t+\Delta t}\mathbf{S},{}^{t+\Delta t}\sigma_{m},{}^{t+\Delta t}\sigma_{y},{}^{t+\Delta t}f)=0 \tag{25}$$

where the yield stress ${}^{t+\Delta}\sigma_{y}$ is related to ${}^{t+\Delta t}\bar{e}^{P}$ by the yield curve of the material,

$${}^{t+\Delta t}\sigma_{y}={}^{t+\Delta t}\sigma_{y}({}^{t}\bar{e}^{P}+\Delta\bar{e}^{P}) \tag{26}$$

In order to satisfy the shell condition (15), the constitutive relations for the normal components of the deviatory ${}^{t+\Delta t}\mathbf{S}$ are [22]

$$S_{xx}=\frac{p_{1}e_{xx}^{"}+p_{2}e_{yy}^{"}}{p_{1}^{2}-p_{2}^{2}}\qquad S_{yy}=\frac{p_{2}e_{xx}^{"}+p_{1}e_{yy}^{"}}{p_{1}^{2}-p_{2}^{2}} \tag{27}$$

and also

$${}^{t+\Delta t}S_{zz}=-{}^{t+\Delta t}\sigma_{m}=-{}^{t+\Delta t}S_{xx}-{}^{t+\Delta t}S_{yy} \tag{28}$$

Here we have

$$p_{1}=c_{1}\Delta\lambda+a_{E}\qquad p_{2}=c_{\nu}\Delta\lambda$$

$$e_{xx}^{"}=c_{1}({}^{t+\Delta t}e_{xx}-{}^{t}e_{xx}^{p})-c_{\nu}({}^{t+\Delta t}e_{yy}-{}^{t}e_{yy}^{p})$$

$$e_{yy}^{"}=-c_{\nu}({}^{t+\Delta t}e_{xx}-{}^{t}e_{xx}^{p})+c_{1}({}^{t+\Delta t}e_{yy}-{}^{t}e_{yy}^{p}) \tag{29}$$

with

$$c_{\nu}\frac{1-\nu}{3(1-\nu)}\qquad c_{1}=1-c_{\nu}\qquad a_{E}=\frac{1}{2G}=\frac{1+\nu}{E} \tag{30}$$

where ν, E, G are Poisson's ratio, Young's modulus and the shear modulus, respectively. The constitutive relations for the shear components have the same form as for the 3-D deformation,

$${}^{t+\Delta t}S_{ij}=\frac{{}^{t+\Delta t}S_{ij}^{E}}{1+2G\Delta\lambda}\qquad i\neq j \tag{31}$$

where ${}^{t+\Delta t}S_{ij}^{E}$ corresponds to the elastic solution (no plastic flow in the current time step).

Following the governing parameter method we select the increment of plastic strain Δe^{P}_{m} to be the governing parameter, as the most appropriate. Then, we can calculate Δf from (22) and ${}^{t+\Delta t}f^{*}$ from (3),

$$f^* = \begin{cases} {}^t f + \Delta f & \text{for } {}^t f \le f_c \\ f_c + K_f({}^t f + \Delta f - f_c) & \text{for } {}^t f \ge f_c \end{cases} \tag{32}$$

We next determine the increment of the effective plastic strain $\Delta\bar{e}^P$. Namely, with the selected $\Delta e^P{}_m$ we can iterate on $\Delta\bar{e}^P$ until one of the conditions, (24) or (25), is satisfied. In these iterations we assume $\Delta\bar{e}^P$ and determine ${}^{t+\Delta t}\sigma_y$ from the yield curve (26), then ${}^{t+\Delta t}f_y^{'}$ from (19), $\Delta\lambda$ from (17); and ${}^{t+\Delta t}S_{ij}$ from (27), (28) and (31). Note that in the iteration on $\Delta\bar{e}^P$ we use initially the value ${}^{t+\Delta t}\sigma_m$ equal to

$${}^{t+\Delta t}\sigma_m = {}^{t+\Delta t}\sigma_m^E - c_m \Delta e_m^P \tag{33}$$

where ${}^{t+\Delta t}\sigma_m^E$ represents the elastic mean stress. During the iterations on $\Delta\bar{e}^P$ we enforce the condition (28). Iterations on $\Delta e^P{}_m$ continue until the condition not used for the iterations on $\Delta\bar{e}^P$ is satisfied ((24) or (25)). Table 1 summarizes the computational steps for the stress integration.

Table 1. Computational steps for stress integration

1. Initial values
   ${}^t e^p$, ${}^t\sigma_y$, ${}^t\bar{e}^p$, ${}^t f$, ${}^{t+\Delta t}\sigma$
2. Trial elastic state
   ${}^{t+\Delta t}\sigma^E = C^E({}^{t+\Delta t}e - {}^t e^P)$
   If ${}^{t+\Delta t}f_y({}^{t+\Delta t}\sigma^E, {}^t f^*, {}^t\sigma_y) \le 0$, solution is elastic, go to step 4;
   otherwise, go to step 3
3. Plasticity calculations
   a) Iteration on Δe_m^P
   $\Delta f = 3(1-{}^t f)\Delta e_m^P / (1 + 3\Delta e_m^P)$
   ${}^{t+\Delta t}f^* = {}^t f + \Delta f = f_c + K_f({}^t f + \Delta f - f_c)$
   b) Iteration on $\Delta\bar{e}^P$
   ${}^{t+\Delta t}\sigma_y = {}^{t+\Delta t}\sigma_y({}^t\bar{e}^P + \Delta\bar{e}^P)$
   ${}^{t+\Delta t}f_y^{'}$ - Equation (19)
   $\Delta\lambda = 3\Delta e_m^P / {}^{t+\Delta t}f_y^{'}$
   ${}^{t+\Delta t}S_{ij}$ - Equations (27), (28), (31)
   ${}^{t+\Delta t}\sigma_m = -{}^{t+\Delta t}S_{zz}$
   Check the condition $|{}^{t+\Delta t}f_e| < \varepsilon$ Equation (24)
   Check the condition $|{}^{t+\Delta t}f_y| < \varepsilon$ Equation (25)
4. Next time step
5. Update the variables and go to step 1

The consistent tangent elastic-elastic matrix ${}^{t+\Delta t}\mathbf{C}^{EP}$ can be determined according to the GPM [17], [30] as

$$ {}^{t+\Delta t}\mathbf{C}^{EP} = \left.\frac{\partial {}^{t+\Delta t}\boldsymbol{\sigma}}{\partial {}^{t+\Delta t}\mathbf{e}}\right|_{p=const.} + \frac{\partial {}^{t+\Delta t}\boldsymbol{\sigma}}{\partial {}^{t+\Delta t}p}\frac{\partial {}^{t+\Delta t}p}{\partial {}^{t+\Delta t}\mathbf{e}} \tag{34} $$

where the first term corresponds to constant governing parameter p. As shown above, the governing parameter for the Gurson model is Δe^{P}_{m}. The derivatives $\partial(\Delta e^{p}_{m})/\partial {}^{t+\Delta t}\mathbf{e}$ can be found from the equation obtained by the differentiation of the yield condition (25) with respect to ${}^{t+\Delta t}\mathbf{e}$,

$$ \mathbf{C}^{E}\frac{\partial {}^{t+\Delta t}f}{\partial {}^{t+\Delta t}\boldsymbol{\sigma}} + \left[-\mathbf{C}^{E}\frac{\partial {}^{t+\Delta t}f_{y}}{\partial {}^{t+\Delta t}\boldsymbol{\sigma}}({}^{t+\Delta t}\mathbf{e}^{p})' + \frac{\partial {}^{t+\Delta t}f_{y}}{\partial({}^{t+\Delta t}\overline{e}^{p})}({}^{t+\Delta t}\mathbf{e}^{p})' + {}^{t+\Delta t}f_{y}'\right]\frac{\partial(\Delta e^{p}_{m})}{\partial {}^{t+\Delta t}\mathbf{e}} = 0 \tag{35} $$

where "'" stands for $\partial/\partial(\Delta e^{P}_{m})$. These expressions correspond to the general 3-D deformation, with the explicit forms of the terms given in [19]. In order to employ the 3-D terms we first convert the shell to the general 3-D conditions. After ${}^{t+\Delta t}\mathbf{C}^{EP}$ (33) is evaluated in the local shell coordinate system, the static condensation must be performed to obtain the shell tangent elastic – plastic matrix in this system.

3. EXTENSION TO LARGE STRAINS

We extend the above stress integration procedure to the large strains following Refs. [19] and [31]. Namely, we employ the multiplicative decomposition of the deformation gradient and the logarithmic strains. According to the multiplicative decomposition of the deformation gradient [32], [33] we have

$$ {}^{t}_{0}\mathbf{F} = {}^{t}_{0}\mathbf{F}^{E}\,{}^{t}_{0}\mathbf{F}^{P} \tag{36} $$

where ${}^{t}_{0}\mathbf{F}$, ${}^{t}_{0}\mathbf{F}^{E}$ and ${}^{t}_{0}\mathbf{F}^{P}$ are the deformation gradient, elastic deformation gradient, and plastic deformation gradient, respectively. The deformation gradients used in further calculations ${}^{t+\Delta t}_{0}\mathbf{F}$ and ${}^{t+\Delta t}_{t}\mathbf{F}$ can be calculated by use of the shell geometry interpolation (11),

$$ {}^{t+\Delta t}_{0}\mathbf{F} = \frac{\partial {}^{t+\Delta t}\mathbf{x}}{\partial {}^{0}\mathbf{x}} = {}^{t+\Delta t}\mathbf{J}\,{}^{0}\mathbf{J}^{-1} \tag{37} $$

$$ {}^{t+\Delta t}_{t}\mathbf{F} = \frac{\partial {}^{t+\Delta t}\mathbf{x}}{\partial {}^{0}\mathbf{x}} = {}^{t+\Delta t}\mathbf{J}\,{}^{t}\mathbf{J}^{-1} \tag{38} $$

where $\mathbf{J} = \partial\mathbf{x}/\partial\mathbf{r}$ are the Jacobins of the coordinate transformation

$$ \mathbf{x} = \mathbf{x}(r,s,t) \tag{39} $$

As in case of a general 3-D deformation, we calculate the trial elastic deformation gradient ${}^{t+\Delta t}_{0}\mathbf{F}^{E}_{*}$ as

$$ {}^{t+\Delta t}_{0}\mathbf{F}^{E}_{*} = {}^{t+\Delta t}_{0}\mathbf{F}\,{}^{0}_{t}\mathbf{F}^{P} = {}^{t+\Delta t}_{t}\mathbf{F}\,{}^{t}_{0}\mathbf{F}\,{}^{0}_{t}\mathbf{F}^{P} \tag{40} $$

where ${}^{0}_{t}\mathbf{F}^{P} = ({}^{t}_{0}\mathbf{F}^{P})^{-1}$. The trial elastic left Cauchy-Green deformation tensor ${}^{t+\Delta t}_{0}\mathbf{B}^{E}_{*}$ is [16]

$$ {}^{t+\Delta t}_{0}\mathbf{B}^{E}_{*} = {}^{t+\Delta t}_{0}\mathbf{F}^{E}_{*}\,{}^{t+\Delta t}_{0}\mathbf{F}^{ET}_{*} = {}^{t+\Delta t}_{t}\mathbf{F}^{E}_{*}\,{}^{t}_{0}\mathbf{B}^{E}_{*}\,{}^{t+\Delta t}_{t}\mathbf{F}^{T} \tag{41} $$

and the logarithmic strain tensor ${}^{t+\Delta t}_{0}\mathbf{e}^{E}_{*}$ is

$$ {}^{t+\Delta t}_{0}\mathbf{e}^{E}_{*} = \sum_{A} \ln({}^{t+\Delta t}_{0}\lambda^{E}_{*A})\,{}^{t+\Delta t}\overline{\mathbf{p}}_{A}\,{}^{t+\Delta t}\overline{\mathbf{p}}_{A} \tag{42} $$

where ${}^{t+\Delta t}_{0}\lambda^{E}_{*A}$ and ${}^{t+\Delta t}\overline{\mathbf{p}}_{A}$ are the principal stretches and the principal vectors obtained by the eigen analysis of ${}^{t+\Delta t}_{0}\mathbf{B}^{E}_{*}$. Form ${}^{t+\Delta t}_{0}\mathbf{e}^{E}_{*}$ we determine the trial elastic stress ${}^{t+\Delta t}\boldsymbol{\sigma}^{E}_{*}$

$$ {}^{t+\Delta t}\boldsymbol{\sigma}^{E}_{*} = \mathbf{C}^{E}\,{}^{t+\Delta t}_{0}\mathbf{e}^{E}_{*} \tag{43} $$

corresponding to ${}^{t+\Delta t}\boldsymbol{\sigma}^{\mathbf{E}}$ in step 2 of Table 1. Further computational steps are the same as for the small strain conditions.

After the stress ${}^{t+\Delta t}\boldsymbol{\sigma}$ has been determined, we need to update the left Cauchy-Green tensor ${}^{t+\Delta t}_{0}\mathbf{B}$. We calculate the elastic strains as

$$ {}^{t+\Delta t}_{0}\mathbf{e}^{E} = \mathbf{C}^{E-1}\,{}^{t+\Delta t}\boldsymbol{\sigma} \tag{44} $$

and then find ${}^{t+\Delta t}_{0}\mathbf{B}^{E}$ as

$$ {}^{t+\Delta t}_{0}\mathbf{B}^{E} = \sum \exp(2\,{}^{t+\Delta t}_{0}e^{E}_{A})\,{}^{t+\Delta t}\mathbf{p}^{E}_{A}\,{}^{t+\Delta t}\mathbf{p}^{E}_{A} \tag{45} $$

where ${}^{t+\Delta t}_{0}e^{E}_{A}$ and ${}^{t+\Delta t}\mathbf{p}^{E}_{A}$ are the principal strains and principal vectors corresponding to the elastic strains ${}^{t+\Delta t}_{0}\mathbf{e}^{E}$ (44). Using this procedure for calculation of ${}^{t+\Delta t}_{0}\mathbf{B}^{E}$ we properly follow the condition (15).

Change of the shell thickness must be taken into account in the large strain shell deformation. With the use of the logarithmic strain definition, we obtain that the shell thickness at the end of time step ${}^{t+\Delta t}a$, is

$$ {}^{t+\Delta t}a = {}^{t}a\exp(\Delta e_{33}) \tag{46} $$

where Δe_{33} is the strain increment in the shell normal direction.

The calculation of the tangent elastic-plastic matrix may be performed as for the small strain conditions. The improvement of the tangent character of this matrix can be achieved by adding the part corresponding to proper differentiations of the geometrical terms, e.g. [34].

4. EXAMPLES

4.1 Necking of a thin sheet

A thin sheet, with very small imperfection progressing from the ends toward the sample central cross-section, is loaded axially. Two FE models are employed: (1) 3-D solid element model, and (2) shell element model. The geometrical data are as given in [35] and [36]. Material data are given in Fig.2(a). One quarter of the sample is modelled due to symmetry.

We have solved this problem by 150 equal steps with prescribed displacements of the sample end. The final deformed configuration for the shell model is shown in Fig.2(a). The force-end displacement diagram is shown in Fig. 2(b). Figure 2(c) shows change of porosity during deformation at the central cross-section of the sample (porosity at the points on the central line is practically the same).

The results obtained by the both FE models are the same, demonstrating the correctness and accuracy of the proposed algorithm for the shell conditions.

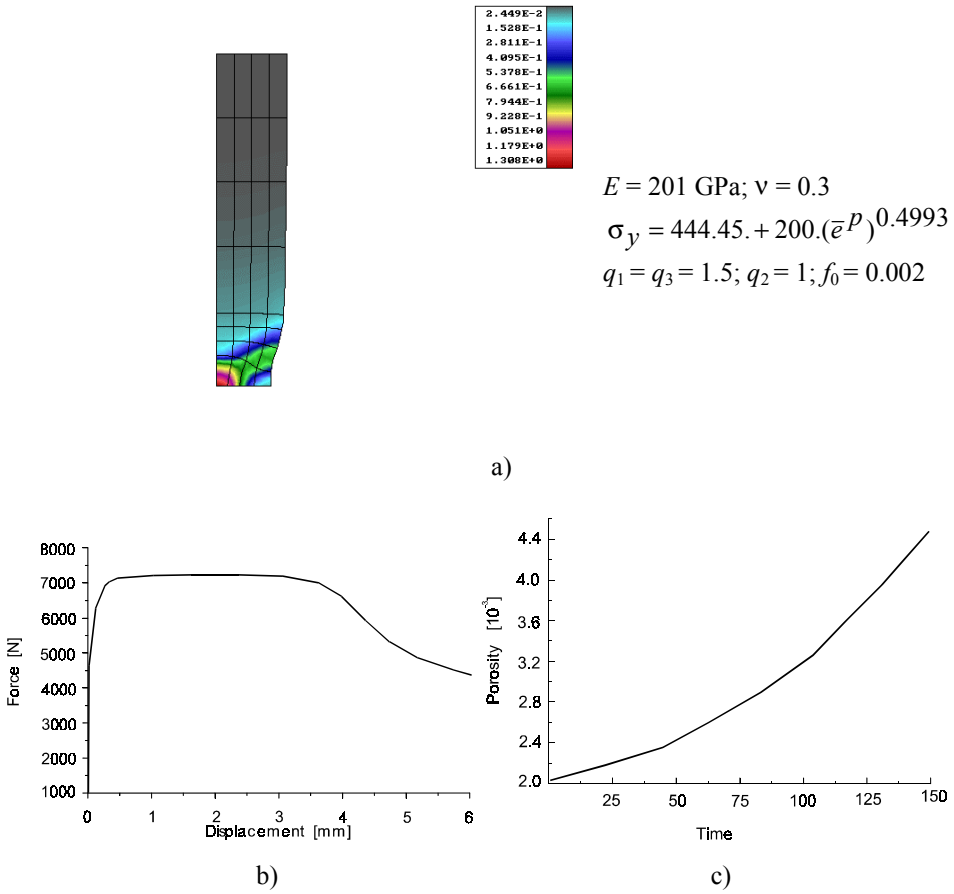

Fig. 2. Necking of a thin sheet:
a) Deformed configuration for the shell model with the field of effective plastic strain
b) Force-displacement dependence
c) Change of porosity in the central cross-section

4.2 Plastic bulging of a circular plate under pressure

A circular plate connected to the rigid wall by the hinge at the outer radius is subjected to the normal pressure increasing with time. The geometrical and the material data are as follows:

R = 24 mm, δ = 1.00 mm

E = 68 Gpa , $\sigma_y = 144.45. + 200.(\bar{e}^p)^{0.5993}$, ν=0.3, $q_1 = q_3 = 1.5$; $q_2 = 1$; $f_o = 0.002$

The final solution is obtained by using 100 constant increments of pressure. The final deformed configuration, with the field of the vertical displacement is shown in Fig.3 (a), while the dependence of the pressure on displacement and change of porosity during deformation of the central point are given in Figs. 3(b), (c), respectively.

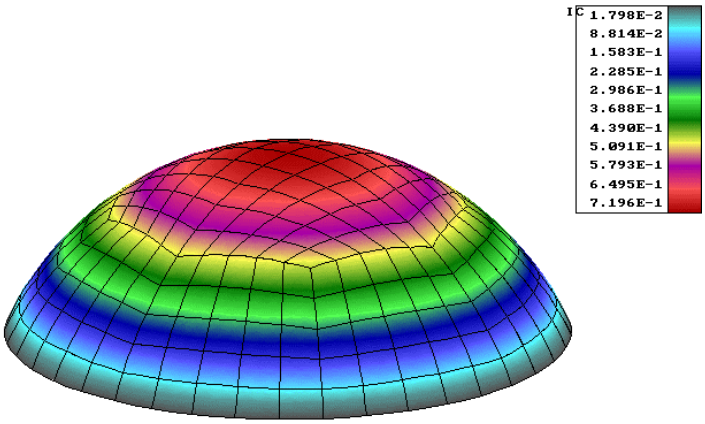

a)

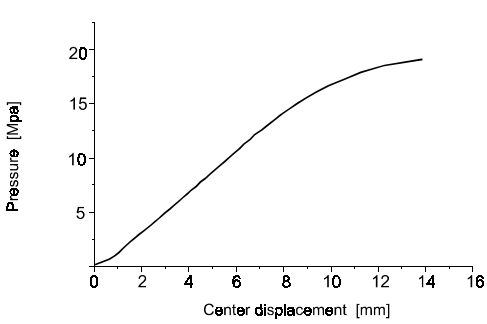

b)

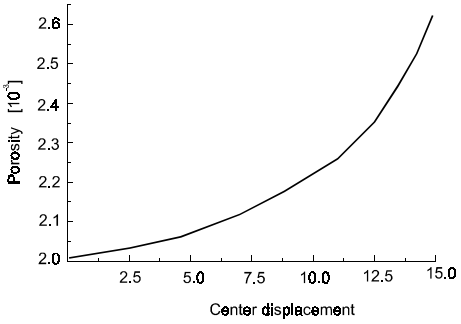

c)

Fig. 3. Plastic bulging of a circular plate
a) Deformed configuration with the field of vertical displacement
b) Pressure - central displacement dependence
c) Change of porosity at the central point

This example was also solved using 2-D axisymmetric FE model, with the large strain formulation [19], and the same solution was obtained. Since the two FE formulations (3-D shell and axisymmetric finite elements) are different, the agreement between the results shows the correctness of the shell solution.

4.3 The tension of plate with hole

The plate of unit thickness with geometrical and material data shown in Fig. 4 a) is subjected to a uniform tension at two sides. Due to symmetry in geometry, boundary conditions and loading, only one-quarter is modelled using 8-node shell (plane stress).

The solution is obtained by using prescribed displacements of the plate edge with the 30 equal increments $\Delta u_y = 0.01$ mm per step. Figure 4 b) shows the final deformed configuration with the effective stress field. The effective plastic strain and porosity at the point B during loading as functions of time (load) steps are shown in Figs. 4 c) and d), respectively.

Table 2 shows unbalanced energy and unbalanced force during equilibrium iterations. The same results are obtained by implementing the 3-D finite element model.

Table 2. Unbalanced energy during equilibrium iterations (step 30)

Iteration	Unbalanced energy	Unbalanced force
1	$17.14\ 10^{0}$	5.24
2	$8.33\ 10^{-2}$	$2.28\ 10^{-2}$
3	$5.162\ 10^{-4}$	$1.05\ 10^{-2}$
4	$9.10\ 10^{-5}$	$3.47\ 10^{-3}$

5. CONCLUDING REMARKS

We have proposed a computational algorithm for stress integration for the Gurson model and the shell deformation. The algorithm represents a simple modification of the one for the general 3-D deformation [19] to include the condition of the zero-stress through the shell thickness. The robustness, accuracy and efficiency of the 3-D algorithm is retained. Computation of the consistent tangent elastic-plastic matrix is the same as for the 3-D conditions, except that the shell solution has to be converted first to these general conditions, and then the static condensation must be applied.

A straightforward extension of the small strain algorithm to the large strain shell deformation is proposed. This simplicity relies on the simple modification of the 3-D large strain kinematics of deformation to the shell FE assumptions. Following this approach, the algorithm based on the multiplicative decomposition of the deformation gradient and on the logarithmic strains is developed.

The solved numerical examples verify the proposed numerical procedure.

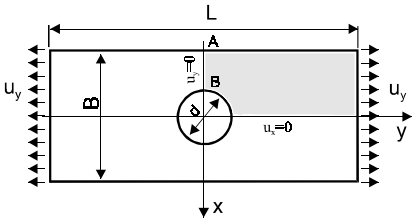

$E = 201$ GPa; $\nu = 0.3$,

$\sigma_y = 444.45. + 200.(\bar{e}^p)^{0.4993}$

$q_1 = q_3 = 1.5$; $q_2 = 1$; $f_0 = 0.002$

L=120 mm B= 20 mm d=10 mm

a)

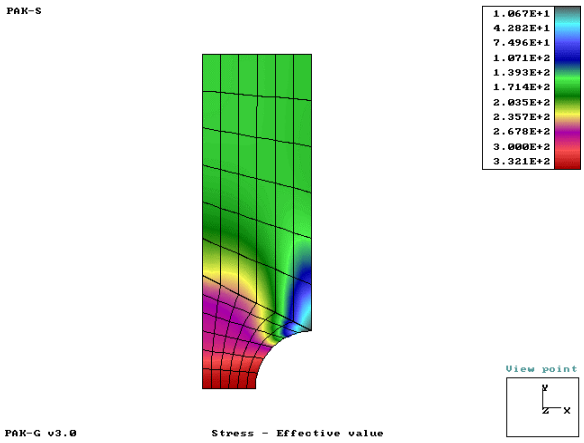

b)

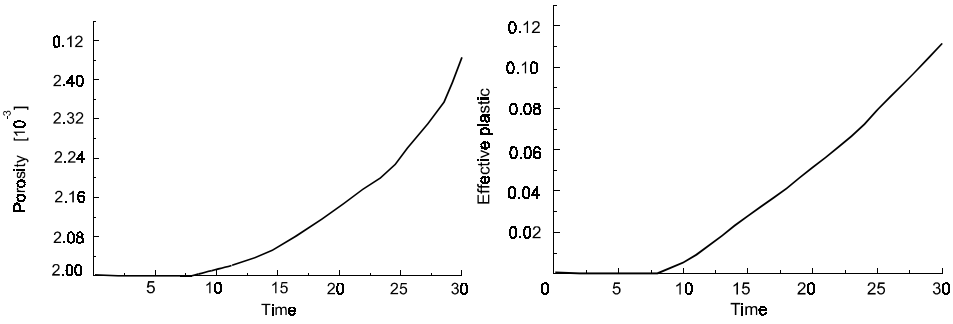

c)

Fig. 4. The tension of plate with a hole
a) Geometrical and material data
b) Deformed configuration with the field of effective stress (step 30)
c) The effective plastic strain and porosity at the point B as functions of time (load) steps

REFERENCES

1. Tresca H (1868) Memoire us I'ecoulement des corps solides. Mem. Pres. Par div. Savants 18, 733-99
2. von Mises R (1913) Mechanic der festen Koerper in Plastisch deformablem Zustand. Goettinger Nachr. Math. Phys.. KI, 582-592
3. Hill R (1950) The Mathematical Theory of Plasticity, Oxford University press London
4. Desai CS, Siriwardane HJ (1984) Constitutive Laws for Engineering Materials, Prentice-Hall Englewood NJ
5. Chen WF, Mizuno E (1990) Nonlinear Analysis in Soil Mechanics, Elsevier Amsterdam
6. Wood DM (1994) Soil Behaviour and Critical State Soil Mechanics, Cambridge University Press Cambridge
7. Cristesu N D , Goida G (1994)Visco-Plastic Behaviour of Geomaterials, Springer-Verlag Wien - New York
8. Mendelson (1968). Plasticity: Theory and Application, The Macmillan Co., New York
9. Penny R K, Marriott DL (1971) Design for Creep, McGraw-Hill Book Co,, Ltd., London
10. Owen DRJ, Hinton E (1978) Finite elements in Plasticity, Pineridge Press Swansea, U. K
11. Chen F, Han DJ (1988) Plasticity for Structural Engineers, Springer-Verlag New York
12. Gurson L (1977) Continuum theory of ductile rupture by void nucleation and growth: Part I – yield criteria and flow rules for porous ductile media 99, 2-15
13. Tvergaard V (1981) Influence of voids on shear band instabilities under plane strain conditions. Int J. Fracture 17, 389-407
14. Tvergaard V (1982) 'On localization in ductile materials containing spherical voids. Int. J. Fracture 18, 237-252
15. Ilyushin AA (1946) Some problems in the theory of plastic deformation. Prikladnaia Mathematika and Mechanika 7, 245-272, 1943 (English translation, RMB-12, Grad. Div. Appl. Math., Rown Univ.
16. Simo JC, Hughes T. J. R. (1998) Computational Inelasticity, Springer-Verlag NY
17. Kojic, M, Bathe KJ Inelastic Analysis of Solids and Srtuctures, Springer-Verlag, Berlin, (to be published).
18. Kojic M Stress integration procedures for inelastic material models within the finite element method. Appl. Mech. Rev., (to be published)
19. Kojic M, Vlastelica I and Zivkovic M (2002) Implicit stress integration procedure for small and large strains of the Gurson material model. Int. J. Numer. Meth. Enging 53, 2701-2720
20. Kojic M (1996) The governing parameter method for implicit integration of viscoplastic constitutive relations for isotropic and orthotropic metals. Computationals Mechanics 19, 49-57
21. Kojic M, Bathe KJ (1987a) The effective-stress-function algorithm for thermo-elastic-plasticity and creep. Int J Numer Method Eng 24, 1509-1532
22. Kojic M, Bathe KJ (1987b) Thermo-elastic-plastic and creep analysis of shell structures. Comput Struct. 26, 135-143
23. Brunet M, Sabourin F (1996) Simulation of necking using damage mechanics in 3-D. sheet metal forming analysis. in J. K. Lee, G. L. Kinzel, and R. H. Wagoner (eds.), Numisheet '96, Proc. 3rd Int. Conf. , Deaborn, MI, 212-219
24. Lee JH, Zhang Y (1994) A finite-element work-hardening plasticity model of uniaxial compression and subsequent failure of porous cylinders including effect of void nucleation and growth - part I: plastic flow and damage. J. Engng. Mater. Technol, 116, 69-79
25. Chu, Needleman A (1986) Void nucleation effects in biaxially stretched sheets. J. Engng. Mater. Technol., Trans. ASME 102, 249-256
26. Bathe KJ 1996 Finite Element Procedures, Prentice Hall, Englewood Cliffs N. J.
27. Kojic M, Slavkovic R, Zivkovic M, Grujovic N (1998) Finite Element Method I – Linear Analysis (in Serbian), Faculty of Mech. Engng., Univ. Kragujevac, Serbia
28. Slavkovic R, Zivkovic M, Kojic M (1994) Enhanced 8-node three-dimensional solid and 4-node shell elements with incompatible generalized displacements. Commun Numer Method Eng 10, 699-709
29. Tvergaard V (1987) Effect of yield surface curvature and void nucleation on plastic flow localization. J. Mech. Phys. Solids 35, 43-60
30. Kojic M (1997) Computational Procedures in Inelastic Analysis of Solids and Structures, Center Sci Res Serbian Academy Sci Art and Univ Kragujevac, Kragujevac, Serbia
31. Kojic M A large strain inelastic analysis of shells based on the multiplicative decomposition of the deformation gradient and the GPM procedure for stress integration. submitted.
32. Lee E. H. (1969) Elastic-Plastic Deformation at Finite Strains. J Appl Mech ASME 36, 1-6

33. Lee EH, Liu DT (1967) Finite strain elastic-plastic theory particularly for plane wave analysis. J Appl Phys 38, 19-28
34. Simo JC, Meschke G (1993). A new class of algorithms for classical plasticity extended to finite strains. Application to geomaterials. Computational Mechanics 11, 253-278
35. Peric Dj, Owen DRJ, Honnor ME (1992) A model for finite strain elastic-plasticity based on logarithmic strains: Computational issues.Compt. Meth. Appl. Mech. Engng. 94, 35-61
36. Ibrahimbegovic A (1994) Finite elastoplastic deformations of space-curved membranes. Compt. Meth. Appl. Mech. Engng. 119, 371-394

ALGORITAM IMPLICITNE INTEGRACIJE NAPONA ZA GURSONOV MODEL U SLUČAJU DEFORMACIJE LJUSKI SA VELIKIM M DILATACIJAMA

Miloš Kojić, Ivo Vlastelica, Miroslav Živković

U radu se izlaze implicitni postupak integracije napona za Gursonov materijalni model - model plastičnosti metala sa zapreminskom plastičnom deformacijom - i za slučaj velikih deformacija ljuske. Računanje napona se zasniva na metodi osnovnog parametra (GPM), sa priraštajem srednje plastične deformacije Δe^P_m uzetim za osnovni parametar. Uslov za napon u ljusci (normalni napon u pravcu debljine ljuske jednak nuli) je zadovoljen na kraju vremenskog koraka (koraka opterećenja) i problem je sveden na rešavanje nelinearne jednačine po Δe^P_m. Postupak je robustan i računski efikasan. Konverzija rešenja za ljusku na 3-D uslove omogućava primenu 3-D konsistentne tangentne elastično-plastične matrice.

Postupak rešavanja za male deformacije je proširen na velike deformacije ljuske. Koriste se multiplikativna dekompozicija gradijenta deformacije i logaritamske deformacije. Ovo proširenje se zasniva na jednostavnoj primeni 3-D kinematičkih relacija na uslove ljuske.

Rešeni numerički primeri ilustruju tačnost i efektivnost predlozenog postupka.

Ključne reči: *Gursonov model, implicitna integracija napona, metod osnovnog parametra, velike deformacije ljuske, multiplikativna dekompozicija gradijenta deformacije, logaritamske deformacije.*